Figures and figure supplements

Visualizing formation of the active site in the mitochondrial ribosome

Viswanathan Chandrasekaran *et al*

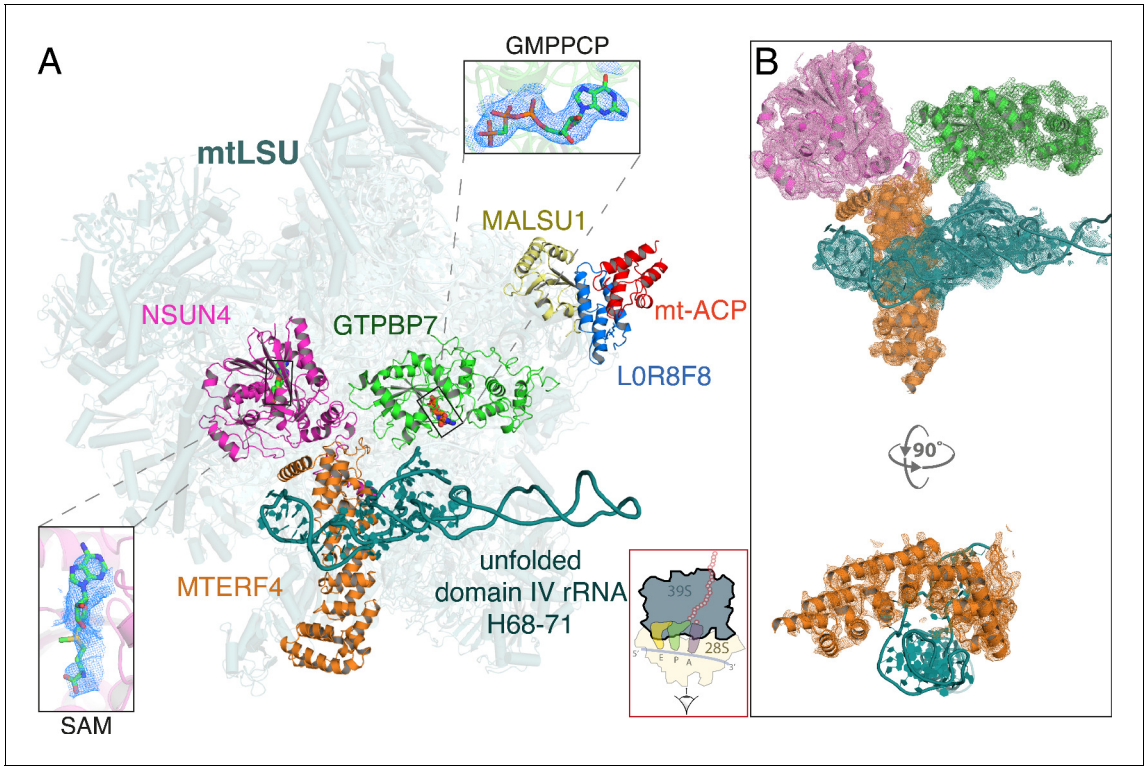

Figure 1. Architecture of the mitoribosomal LSU complexed with NSUN4·MTERF4·GTPBP7·GMPPCP and MALSU1-L0R8F8-mt-ACP. (**A**) The inter-subunit interface faces the reader and a cartoon of an elongating mitoribosome is shown in the red box (bottom) to aid orientation. NSUN4 (pink) bound to S-adenosyl methionine (SAM, left inset), GTPBP7 (green) bound to the non-hydrolyzable GTP analog, GMPPCP (top inset) and MTERF4 (orange) interact with the subunit interface of the mtLSU assembly intermediate. The domain IV rRNA helices H68-71 (teal) are unfolded, rendering the aminoacyl, peptidyl, and exit sites incomplete. Also pictured are the anti-association factors MALSU1 (yellow), L0R8F8 (blue), and mt-ACP (red). (**B**) Map-to-model fits for NSUN4, MTERF4, GTPBP7, and the unfolded rRNA.

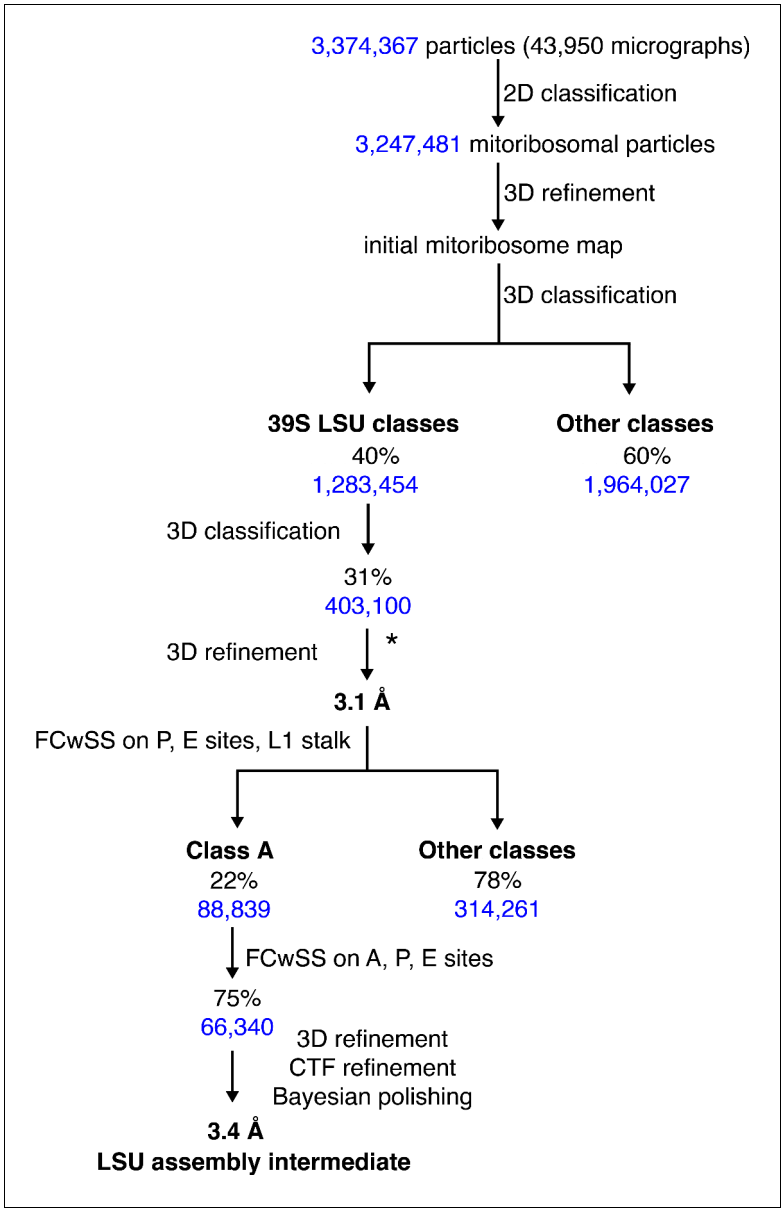

Figure 1—figure supplement 1. Cryo-EM analysis of human mitoribosomes Data processing scheme. * indicates that the particles were re-extracted to 1.04 Å/pixel. cryo-EM, cryo-electron microscopy.

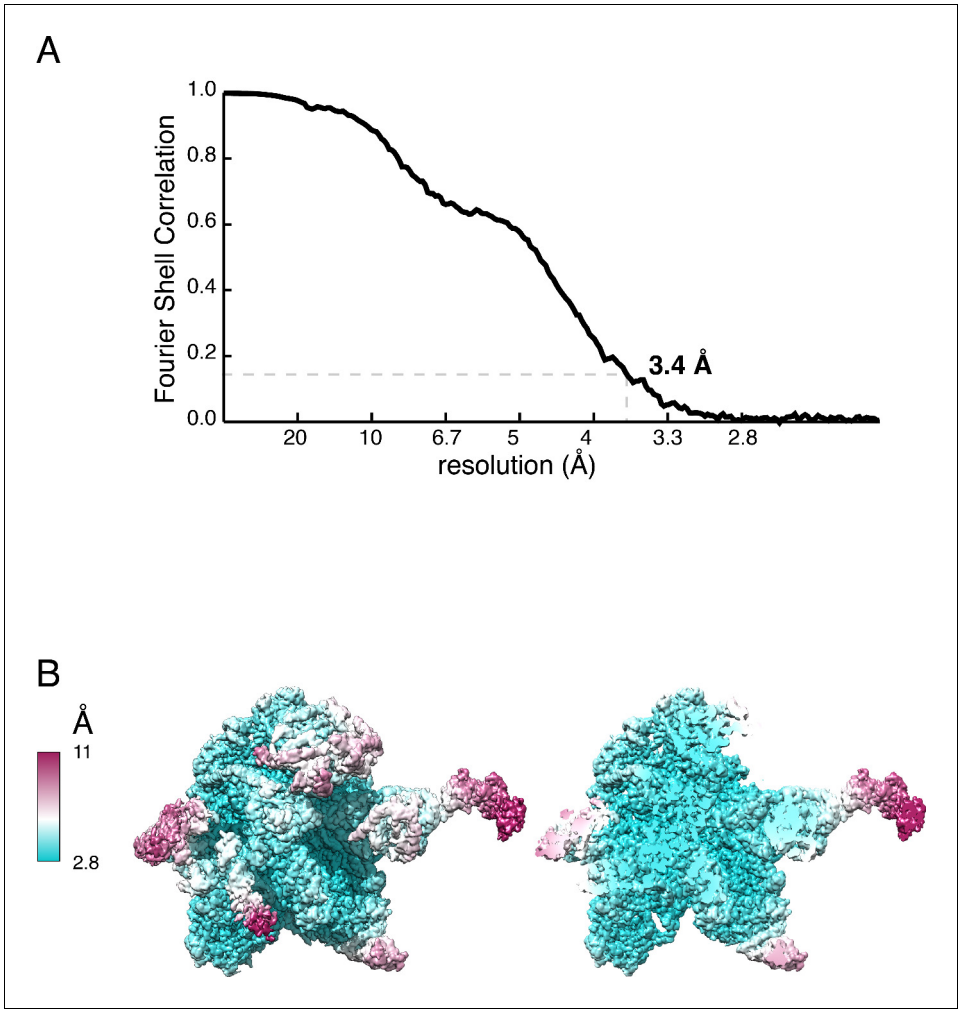

Figure 1—figure supplement 2. Gold-standard FSC curve (**A**) and local resolution (**B**) of the mtLSU assembly intermediate map. FSC, Fourier shell correlation; mtLSU, mitoribosomal large subunit.

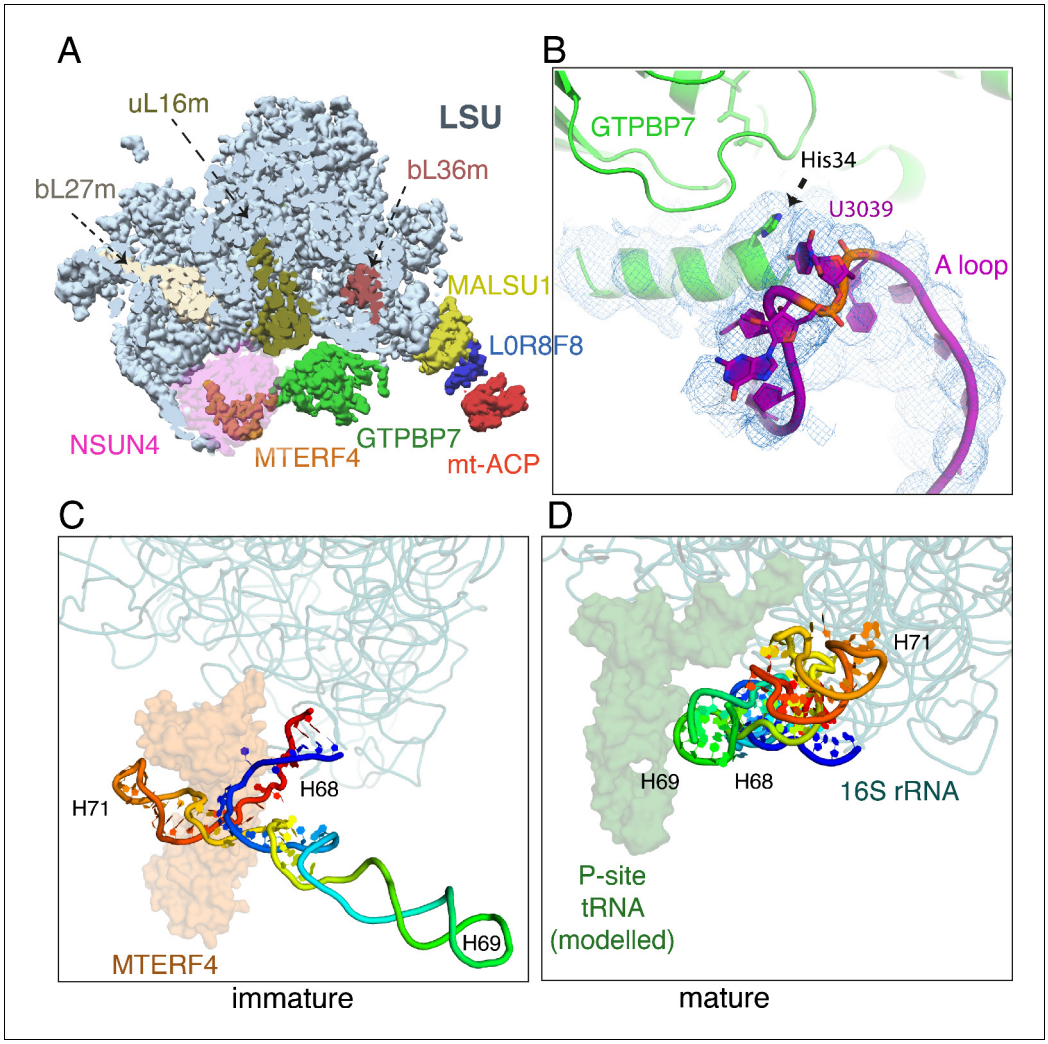

Figure 2. Maturation of the mtLSU by NSUN4·MTERF4·GTPBP7. (**A**) Incorporation of uL16m (olive), bL27m (wheat) precedes NSUN4 (magenta) binding and before bL36m (brown). NSUN4 is shown translucent for clarity. (**B**) His34 of helix 1 of GTPBP7 verifies that 2′-O-methylation of A-loop base U3039 by MRM2 has occurred. Immature (**C**) and mature (**D**) conformations of domain IV rRNA helices H68–71 (rainbow). H69 would pack against a canonical P-site tRNA when present, and together this region forms the back wall of the A, P, and E sites of the mature 39S. MTERF4 (translucent orange) holds H68–71 in an unfolded conformation to permit assembly factors to access the core of the mtLSU. mtLSU, mitoribosomal large subunit; rRNA, ribosomal RNA.

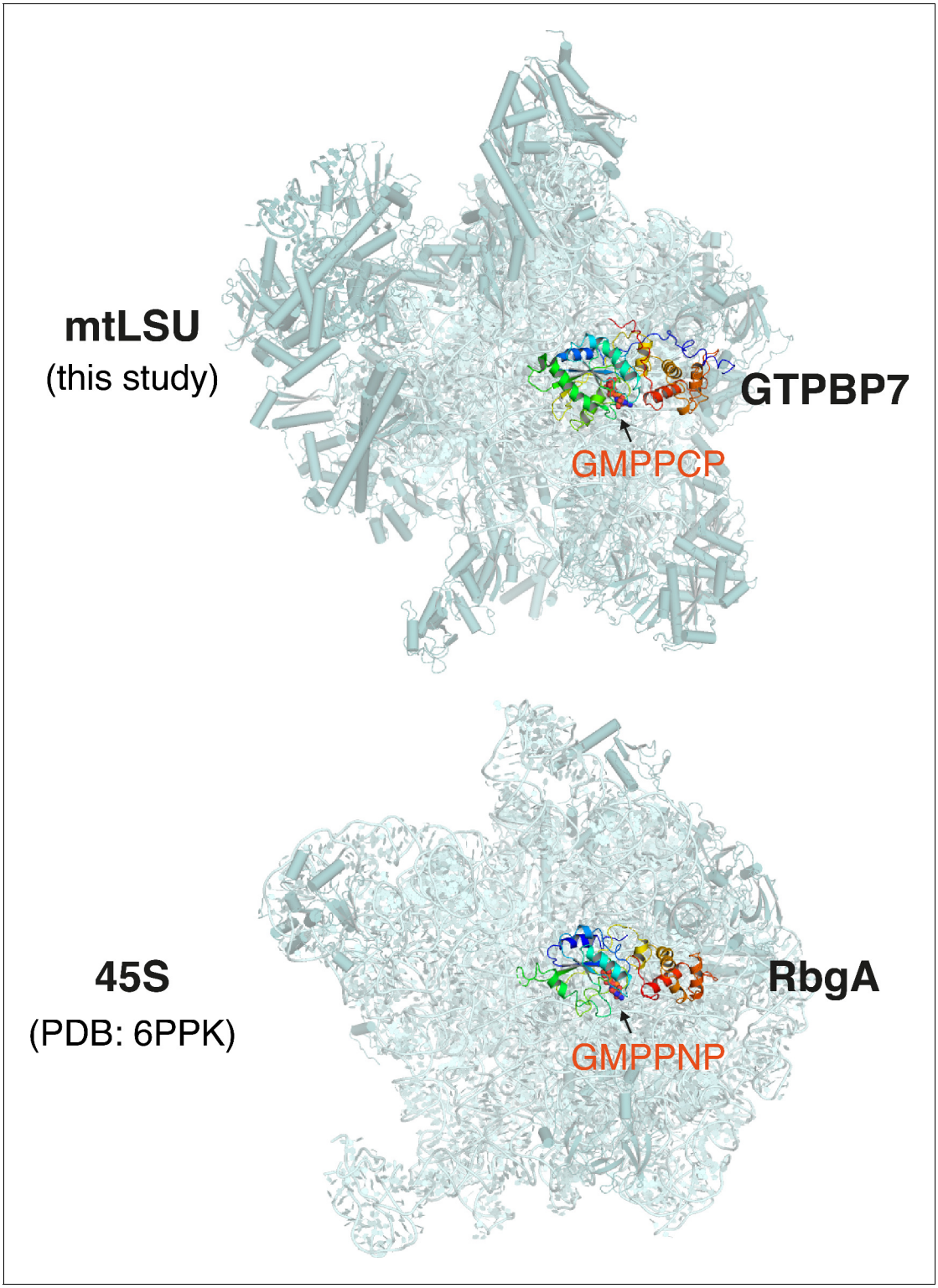

Figure 2—figure supplement 1. Comparison of MTG1-bound human mtLSU and RbgA-bound *Bacillus subtilis* 45S. The inter-subunit interface is oriented toward the reader. GTPBP7 (top) or RbgA (bottom) bound to the non-hydrolyzable GTP analogs, GMPPCP (top) or GMPPNP (bottom) interact at equivalent locations on the human mtLSU and bacterial 45S, respectively. mtLSU, mitoribosomal large subunit.

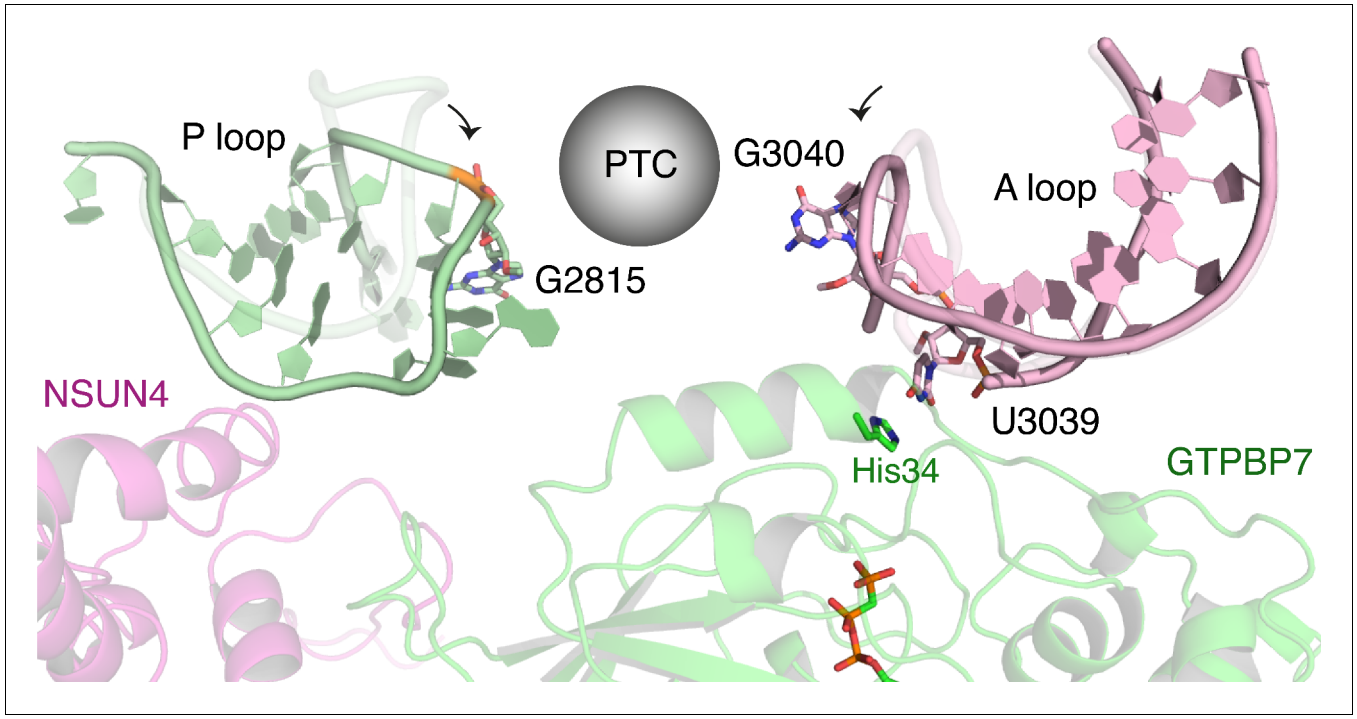

Figure 2—figure supplement 2. GTPBP7 binds directly to the A loop of the 16S rRNA. The tips of the A and P loops move toward GTPBP7 and NSUN4 relative to their positions in the mature mitoribosomes (overlaid in translucent colors). rRNA, ribosomal RNA.

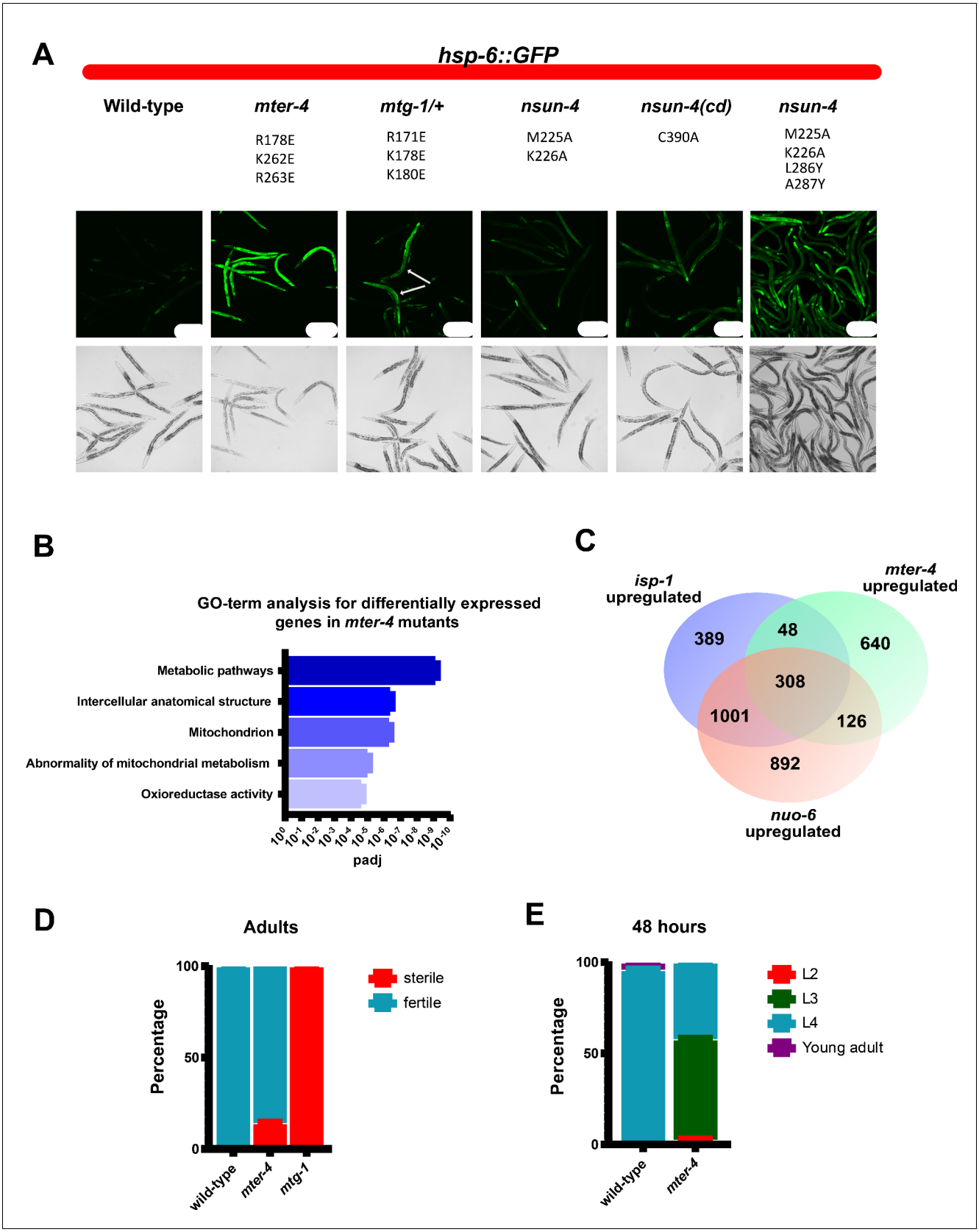

Figure 3. Mutations that disrupt mitoribosomal LSU binding result in activation of the mitochondrial unfolded protein response, delayed development, and decreased fertility. (**A**) Representative images of hsp-6::GFP expression in wild-type, *mter-4*^{R178E,K262E,K263E}, *mtg-1*^{R171E,K178E,K180E}, *nsun-4*^{M225A,K226A},

Figure 3 continued on next page

Figure 3 continued

catalytic dead *nsun-4*^{C90A}, and *nsun-4*^{M225A,K226A,L286Y,A287Y} mutant animals. The matched wild-type control for *nsun-4*^{M225A,K226A,L286Y,A287Y} resembles the shown wild-type, and is omitted for simplicity. White arrows in mtg-1 mutants represent homozygous mutant animals based on the absence of *umnIs21* reporter expression from balancer chromosome. All animals express the *zcls13 [hsp-6::GFP]* reporter which is specifically expressed in response to mitochondrial stress. Animals were grown for 72 hr at 22.5˚C. Scale bars=200 μm. (**B**) Top five GO-terms based on p-value from g:Profiler analysis of genes upregulated greater than 0.5 (log2) in *mter-4*^{R178E,K262E,K263E} mutants when compared to wild-type animals. (**C**) Venn diagram comparison of genes upregulated in *mter-4*^{R178E,K262E,K263E}, *isp-1(qmv150)*, and *nuo-6(qm200)* mutants. *isp-1* and *nuo-6* gene expression data from ***Yee et al., 2014***. (**D**) Fraction of wild-type and *mter-4*^{R178E,K262E,K263E} mutants sterile at 22.5˚C. n=100 animals. (**E**) Fraction of wild-type and *mter-4*^{R178E,K262E,K263E} mutants at different developmental stages after 48 hr at 22.5˚C. n=200 animals. GO, gene ontology.

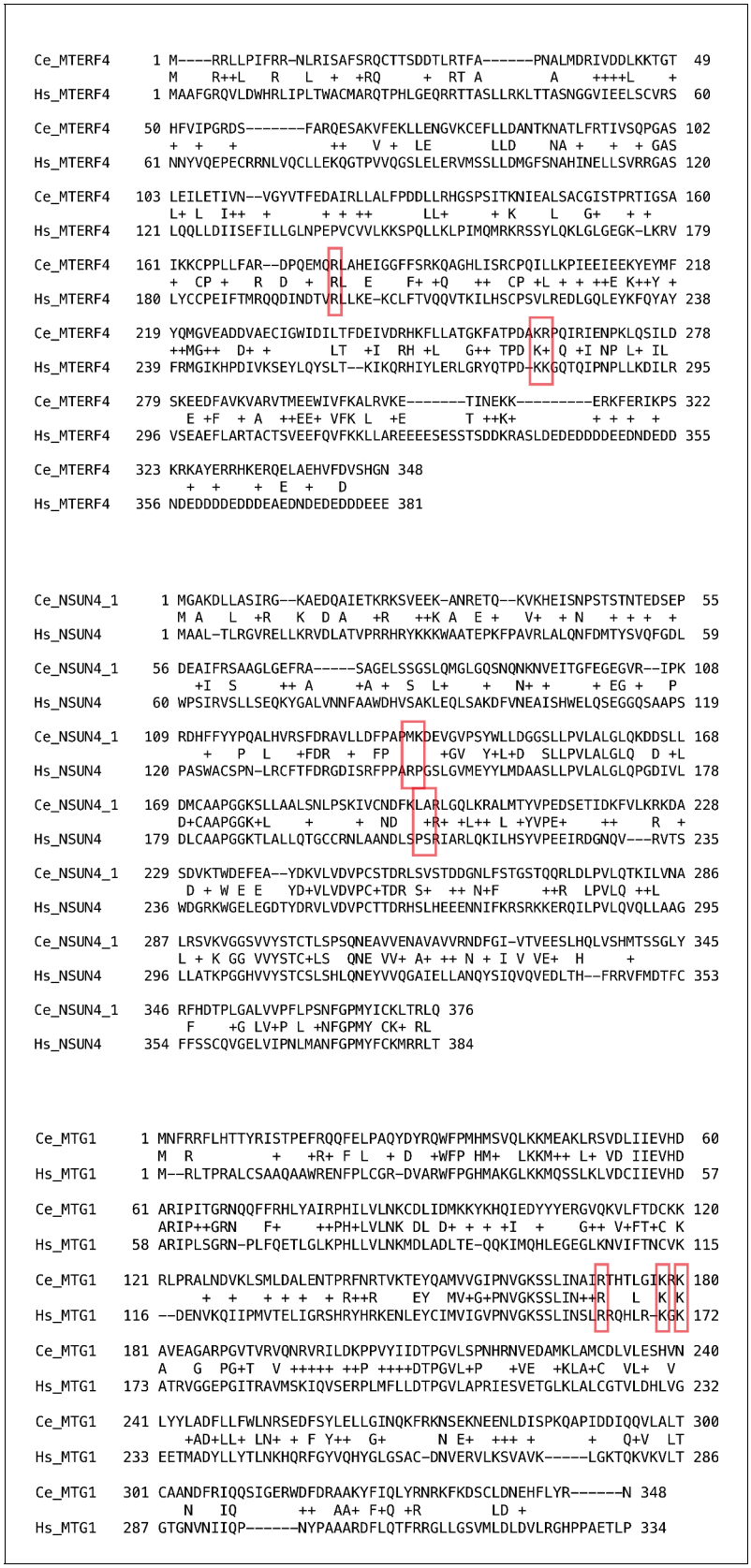

Figure 3—figure supplement 1. Sequence alignments of *Caenorhabditis elegans* (Ce) and human (Hs) MTERF4 (top), NSUN4 (middle), and GTPBP7 (MTG1, bottom). Residues that are important for mitoribosome binding and that were mutated in this study are highlighted in red.

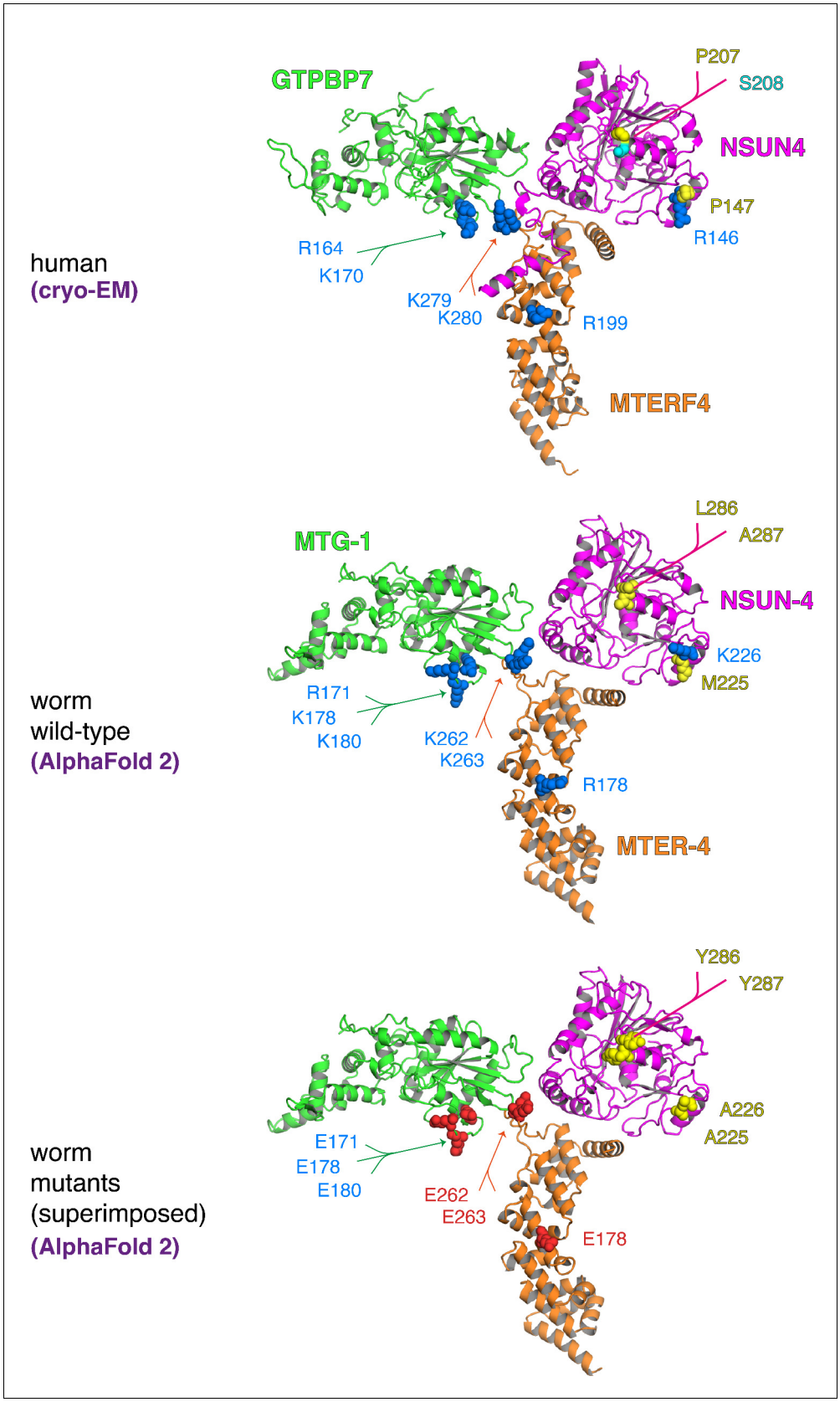

Figure 3—figure supplement 2. Structural conservation of human and *Caenorhabditis elegans* MTERF4, NSUN4, and GTPBP7. Cryo-EM structure of the human complex (top) and *C. elegans* AlphaFold 2 models of wild-type

Figure 3—figure supplement 2 continued on next page

Figure 3—figure supplement 2 continued

(middle) and mutant (bottom) MTERF4 (orange), NSUN4 (magenta) and GTPBP7 (green) illustrate the high degree of structural conservation from human to worm. The introduced mutations in the mitoribosome binding interfaces of the *C. elegans* proteins do not affect the overall fold of the proteins as predicted by AlphaFold 2. Mutated sidechains are depicted as spheres and coloured by type (positive - blue, negative - red, hydrophobic – yellow, polar - cyan). Note that worm strains generated in this study did not carry mutations on all three proteins simultaneously as depicted here.

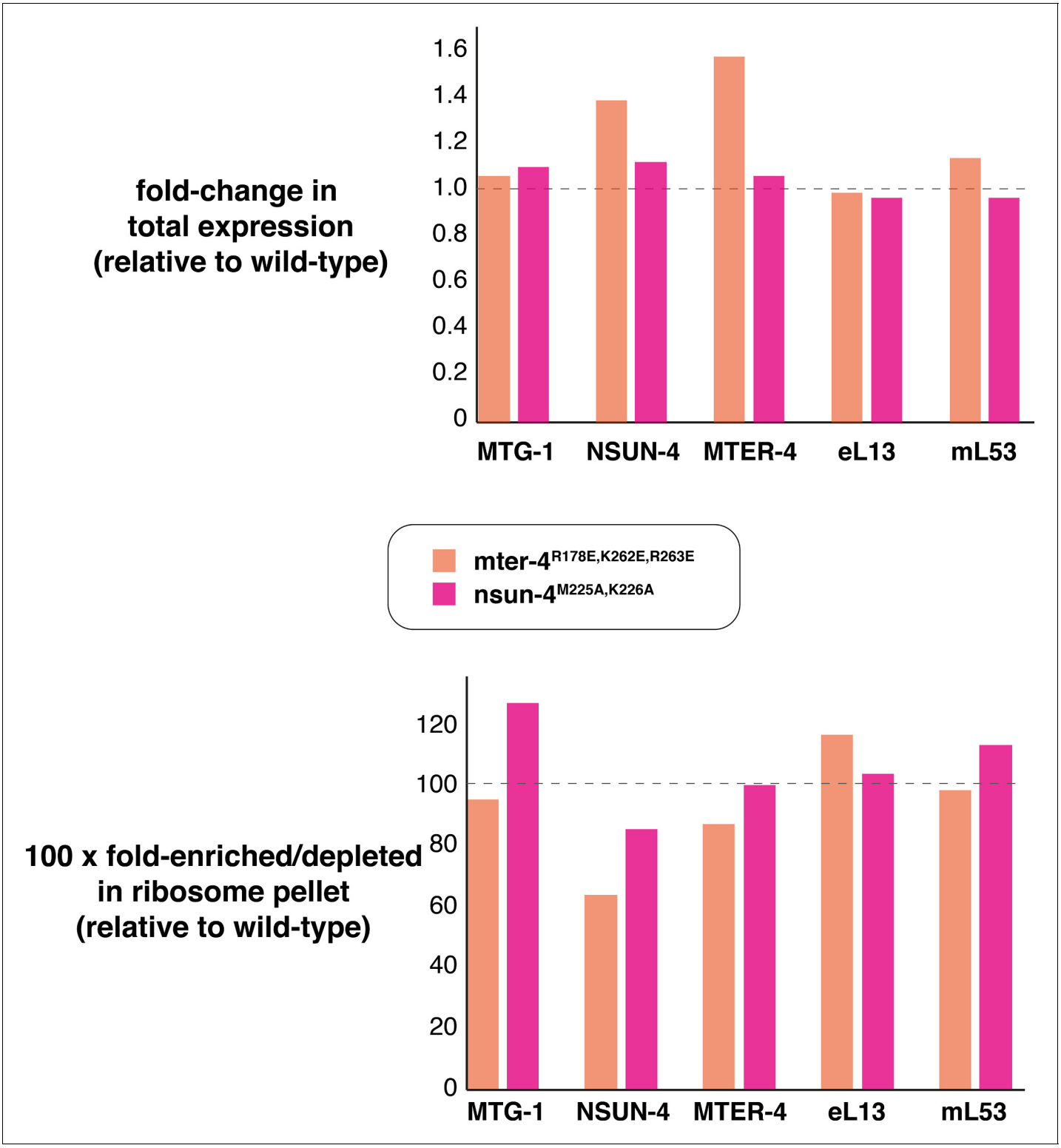

Figure 3—figure supplement 3. TMT-MS quantification of protein levels (top). Total protein levels of MTG-1, NSUN-4, and MTER-4 as well as the cytosolic ribosomal protein eL13 and the mitoribosomal protein mL53 are comparable to those in wild-type worms. Each value is an average of two biological replicates. (bottom) NSUN-4 and MTER-4 are significantly depleted in the ribosomal fraction (which includes cytosolic and mitochondrial ribosomes) in the *mter-4*^{R178E,K262E,R263E} strain and to a lesser extent in the *nsun-4*^{M225A,K226A} strain. TMT-MS, Tandem mass tag-mass spectrometry.

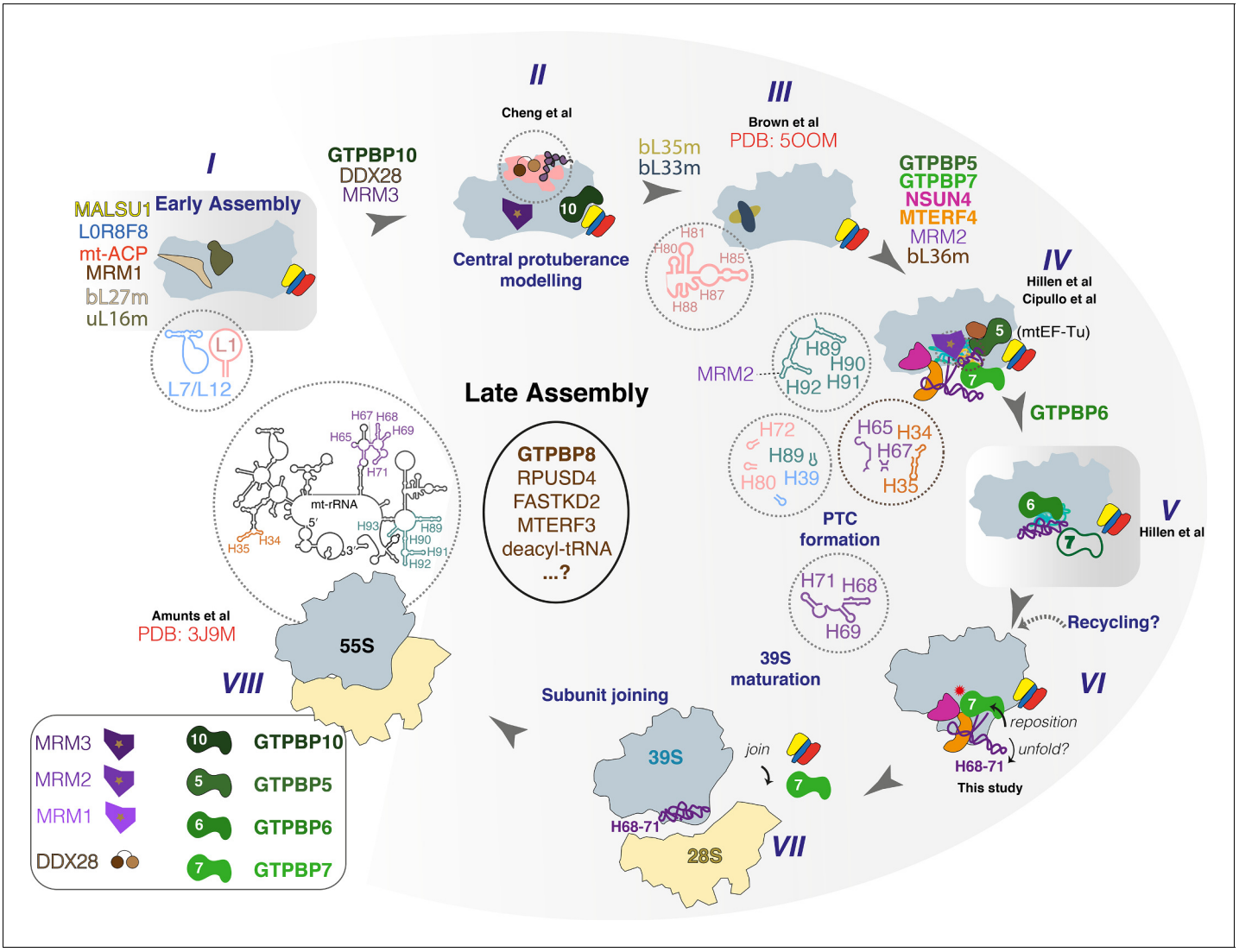

Figure 4. Proposed sequence of events in late-stage mtLSU assembly. States I–VIII along the human mtLSU late-stage maturation pathway, including recently reported states II (***Cheng et al., 2021***), III (***Brown et al., 2017***), IV (***Cipullo et al., 2021***; ***Hillen et al., 2021***), V (***Hillen et al., 2021***), VI (this study), and VIII (***Amunts et al., 2015***). Note that state V was seen only to contain GTPBP6 and GTPBP7 is therefore depicted hollow. mtLSU, mitoribosomal large subunit.